Inductively Coupled Argon Plasma-Enhanced Quantum-Well Intermixing: Cap Layer Effect and Plasma Process Influence

Chengdong Xu and Ting Mei, *Senior Member, IEEE*

***Abstract*—Comprehensive investigation on inductively coupled argon plasma-enhanced quantum-well intermixing is done on an InGaAs–InP quantum-well structure with p-/n- doped InP and InGaAs caps using polarized edge-emitting photoluminescence analysis technique. The derived diffusion lengths on group V and III sublattices show that the cap material plays an important role as it influences both the accumulation and diffusion of point defects during plasma process and annealing process, respectively. The large blue and red shift can be realized with p-InP and n-InGaAs caps, respectively, by controlling the diffusion length ratio for interdiffusion on two sublattices.**

***Index Terms*—Inductively coupled plasma (ICP), interdiffusion, photonic integrated circuits (PICs), quantum wells (QWs), quantum-well intermixing (QWI).**

I. Introduction

FOR decades, the topic of quantum-well intermixing (QWI) has been attracting considerable research efforts due to its potential in modifying bandgap energy across a single substrate in postgrowth-level process, which offers an easy and reliable approach for monolithically integrating various types of photonic devices on III-V compound semiconductor-based material platforms. Over its development history, a number of techniques, such as impurity-free vacancy disordering (IFVD) [1], laser-induced disordering [2], ion-implantation-induced disordering (IIID) [3], low-temperature-grown InP-induced intermixing [4], sputtered SiO_2-induced disordering [5], inductively coupled argon plasma-enhanced (Ar-ICP) intermixing [6], etc., have been demonstrated. IFVD is one of the most successful techniques for the GaAs-based ternary material system and has been adopted for laser array fabrication [7], whereas its performance on the InP-based quaternary material system is accompanied with large thermal shift [8]. The challenge in the latter comes from the material's poor thermal stability that causes large uncontrollable thermal shift [9]. By adopting Ge incorporation in sol-gel derived SiO_2 and intermixing suppression by e-beam-evaporated SiO_2, a 64-nm blue shift was achieved with a small thermal shift [10]. Some special technique was also reported to improve the thermal stability such as adopting a thin GaAs interlayer to minimize As/P exchange [11]. IIID is efficient for the InP-based quaternary material system, which presents large blueshift and small thermal shift; but damage to the material quality is unavoidable even when the control in ion energy [12], [13] has been taken into consideration for process optimization. ICP-enhanced intermixing has been demonstrated as a promising technique for both quantum-well (QW) [14] and quantum-dot (QD) [15] InP-based materials in aspects of controllable large bandgap shift [14], small thermal shift, and material quality preservation [16], [17]. This technique has been applied in monolithic integration. [18]–[21]. In this technique, point defects are deliberately generated near the surface in the argon plasma exposure process and diffuse downwards to promote interdiffusion in the heterostructures via kick-out mechanism [22] during the subsequent annealing. In our previous work, both large blue and red differential shifts were implemented with different cap materials [14], [23]. However, the influence of cap materials and processing conditions on intermixing has yet to be investigated. In this paper, we study these influencing factors for the ICP-enhanced intermixing technique.

Manuscript received September 15, 2008; revised December 02, 2008. Current version published July 01, 2009. This work was supported in part by the Singapore National Research Foundation under CRP Award NRF-G-CRP 2007-01 and by the Ministry of Education (MOE) and the Agency for Science, Technology and Research (A*STAR), Singapore, under Research Grant ARC 2/05.

The authors are with the School of Electrical and Electronic Engineering, Nanyang Technological University, Singapore, Singapore 639798 (e-mail: cdxu@main.ntu.edu.sg; etmei@ntu.edu.sg).

Color versions of one or more of the figures in this paper are available online at http://ieeexplore.ieee.org.

Digital Object Identifier 10.1109/JQE.2009.2014649

II. Experimental Procedure

The ICP-enhanced intermixing involves two processing steps: the argon plasma exposure for modifying the near-surface lattice of the cap layer and the rapid thermal annealing (RTA) for promoting intermixing. The enhancement of intermixing is due to point defects generated near the surface of the cap layer. Therefore, a thorough investigation is necessary for various materials and doping types of the cap layer. An ideal cap layer should accommodate sufficient point defects for intermixing enhancement and bring no extrinsic atomic species to the samples.

For InGaAsP–InP heterostructures on InP substrate, $In_{0.53}Ga_{0.47}As$ and InP are two natural choices for the cap layer due to their lattice-matching to the substrate. Other possible choices are not adopted in this investigation to avoid complicating the experiment and analysis. The experiment employed four types of samples with these two cap layers being doped in p- and n- types. The lattice-matched $In_{0.53}Ga_{0.47}As$–InP single QW structures were grown by metal–organic vapor phase epitaxy on (100)-oriented n^+-type InP substrates. The 3.5-nm-thick undoped well layer is sandwiched between two 200-nm-thick undoped InP layers. On top of the structure is an 800-nm-thick cap layer of InP or $In_{0.53}Ga_{0.47}As$, doped with p-dopant, Zn or n-dopant, Si to 2×10^{18} cm^{-3}.

The argon ICP processing step was implemented using Plasmalab System 100 by Oxford Instruments. The RTA processing step was performed under flowing N_2 ambient at 550 °C for durations ranging from 30 to 240 s. InP and GaAs proximity caps were used to prevent P outdiffusion for InP capped samples and As outdiffusion for InGaAs capped samples, respectively, during annealing process. The room-temperature photoluminescence (PL) was inspected before and after the process. In this investigation, no thermal shift was observed on all RTA-only samples with temperature less than 550 °C, which implies that samples are thermally stable at this temperature.

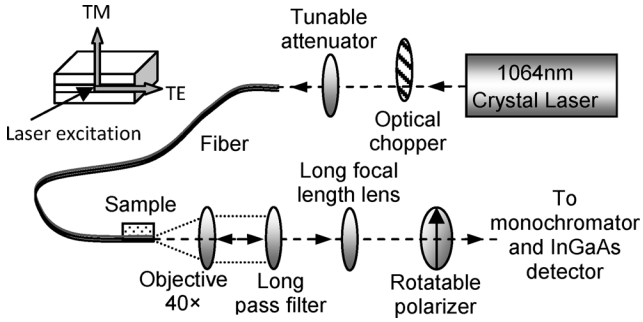

Fig. 1. Schematic diagram of the PPL test setup.

III. Quantitative Characterization

As the important parameter for characterizing heterostructure intermixing, the diffusion length is derived from the shift of the peak wavelength in PL measurement. However, unlike the ternary material system such as AlGaAs/GaAs, a quaternary material system, e.g., InGaAs(P)–InP, may allow interdiffusion on both group V and III sublattices, which results in two diffusion lengths, L_{V} and L_{III}. With conventional PL measurement, the diffusion lengths can be derived only when the diffusion-length ratio, i.e., $k = L_{\mathrm{V}}/L_{\mathrm{III}}$, is presumed, as was done in previous investigation [24]. In past decades, not much attention has been paid to the k effect, whereas it had been commonly believed that k lies between $0.8 \sim 2$ [25]–[29]. However, in our previous experiment presenting the red-shift phenomenon [23], very small k ($\sim$ 0.25) was achieved, implying group III sublattice's interdiffusion length is four times as that of group V' sublattice. The ICP-enhanced intermixing technique is unique in that both blue shift [14] and red shift [23] have been obtained, which indicates that both group V and group III dominant intermixing are possible.

Little investigation on k effect had been done previously due to limitation of the characterization apparatuses. Several methods, such as scanning tunnelling microscopy [25], double crystal X-ray diffractometry [26], high-resolution X-ray diffraction [27], differential reflectance [28], and absorbance measurement [29], were used to estimate the diffusion length ratio. However, these methods are time consuming, demand large sample size, and/or are destructive to samples, and thus are not suitable for investigation involving large test volume.

We have presented the polarized photoluminescence (PPL) technique as an effective way to determine L_{V} and L_{III} [30], which is based on measurement of room-temperature edge-emitting PPL spectra. Fig. 1 shows the experimental setup for the PPL measurement. A 1064 nm diode-pumped solid state laser is used for excitation, whereas the excitation level is adjusted by a tunable attenuator before the light is coupled into a fibre by a 10 × objective lens. The other end of the fiber is fixed in the V-groove of the sample stage and aligned with the facet of the sample under test in the focal plane of a 40 × objective lens. A long pass filter with a reflectance of 98% at 1064 nm and less than 40% within 1200 –1700 nm is placed behind the objective lens. The excitation light is collimated by the objective lens, reflected back by the long pass filter and focused on the sample facet via the same lens. The edge-emitting PL is collimated by the objective lens, passes the long pass filter and is received by the subsequent optical system for spectrum measurement. A rotatable polarizer is used to select the TE- and TM-polarized PL before the monochromator. A TE-cooled InGaAs photodetector is connected to the output port of the monochromator to measure the PL intensity.

Fig. 2 shows typical TE- and TM-polarized PL spectra, from which we see that the electron-heavy-hole (C-HH) and the electron-light-hole (C-LH) transitions present different proportions in the two spectra. Theoretically, the strengths of C-HH and C-LH transition are

$$\left|\left\langle iS\uparrow|p_x|\frac{3}{2},\frac{3}{2}\right\rangle\right|^2=\frac{1}{2}|p_{CV}|^2$$
$$\left|\left\langle iS\uparrow|p_x|\frac{3}{2},\frac{1}{2}\right\rangle\right|^2=\frac{1}{6}|p_{CV}|^2$$

for in-plane (xy) polarization (TE) and

$$\left|\left\langle iS\uparrow|p_z|\frac{3}{2},\frac{3}{2}\right\rangle\right|^2=0$$
$$\left|\left\langle iS\uparrow|p_z|\frac{3}{2},\frac{1}{2}\right\rangle\right|^2=\frac{2}{3}|p_{CV}|^2$$

for z plane polarization (TM) in QWs, where p_{cv} is the transition matrix element between a conduction band with unit cell function $|c>$ and a valence band with unit cell function $|\nu>$. In our experiment, the polarization of incident excitation beam, which influences the degrees of polarization of heavy- and light-hole transitions [31], was not controlled intentionally. The light holes can relax to heavy holes to enhance the C-HH emission, whereas interface roughness may cause depolarization as well. Therefore, the relative intensities as predicted by the above equations cannot be retained in the PL measurement. However, from Fig. 2, it is clear that the PL spectra are highly polarization-dependent, which shows that the C-HH and C-LH emissions have different contributions to the TE- and TM-PPL spectra. The peak wavelengths of C-HH and C-LH transitions can be determined by fitting two-peak Gaussian curves to the TE- and TM- PPL spectra correlatively. As shown in Fig. 3, the C-HH peak wavelength is determined by curve-fitting to the TE-PPL spectrum with fixed C-LH peak wavelength, and the C-LH peak wavelength is determined by curve-fitting to the TM-PPL spectrum with fixed C-HH peak wavelength. A number of iterations of this process are needed before both C-HH and C-LH peak wavelengths are well determined. The fitted spectra of C-HH

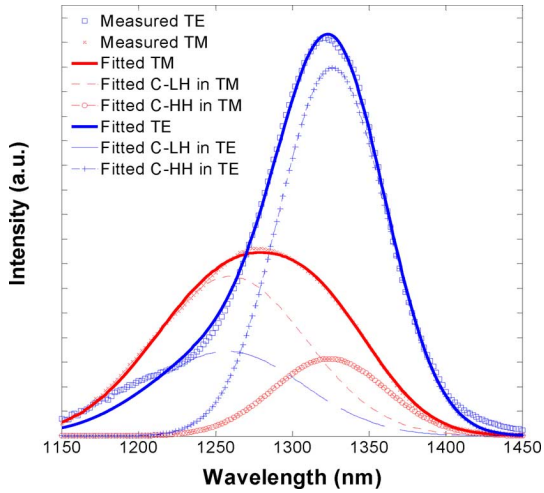

Fig. 2. Measured PPL spectra and fitted curves.

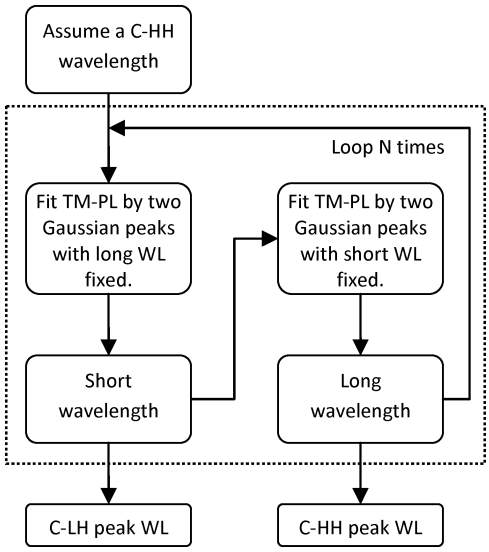

Fig. 3. Flowchart for determining C-HH and C-LH peak wavelengths from TE- and TM-PPL spectra.

and C-LH transitions from TE-and TM-PPL are shown in Fig. 2 as well.

IV. Cap Layer Effect

In this investigation, p-type and n-type InP and $In_{0.53}Ga0_{.47}As$ are adopted as cap layers. Samples were exposed in Ar-plasma for 1 min, with RF power and ICP power set at 400 and 500 W, respectively. The subsequent RTA process was performed for a series of duration from 60 to 180 s at 550 °C. Fig. 4 shows the measured TE- and TM-PPL spectra for a series of annealing durations for samples with p-/ n- InP and $In_{0.53}Ga0_{.47}As$ cap layers. Fig. 5 shows the wavelength shifts of C-HH and C-LH transitions, and Fig. 6 shows the derived L_V and L_{III} accordingly.

Apparently, the p-InP capped sample achieves much higher blue shift than the n-InP capped sample, especially for short RTA duration. The achieved blue shift for p-InGaAs capped sample is much smaller than that for the p-InP capped sample even with long annealing duration, whereas red shift has been

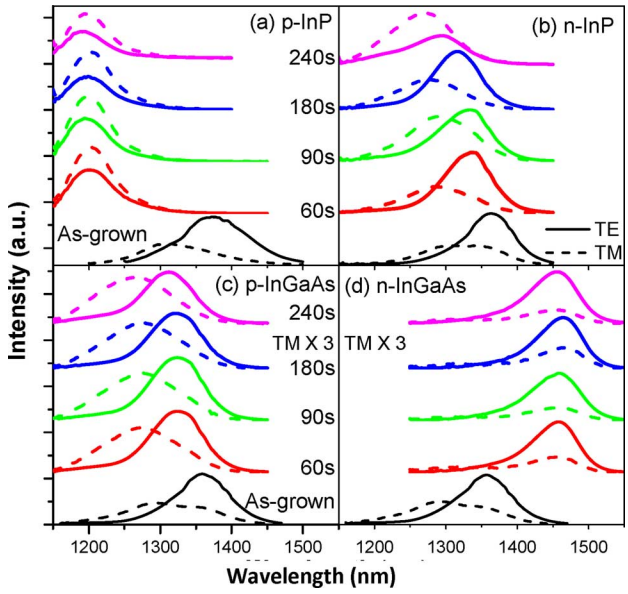

Fig. 4. Measured TE- and TM-PPL spectra for different annealing durations.

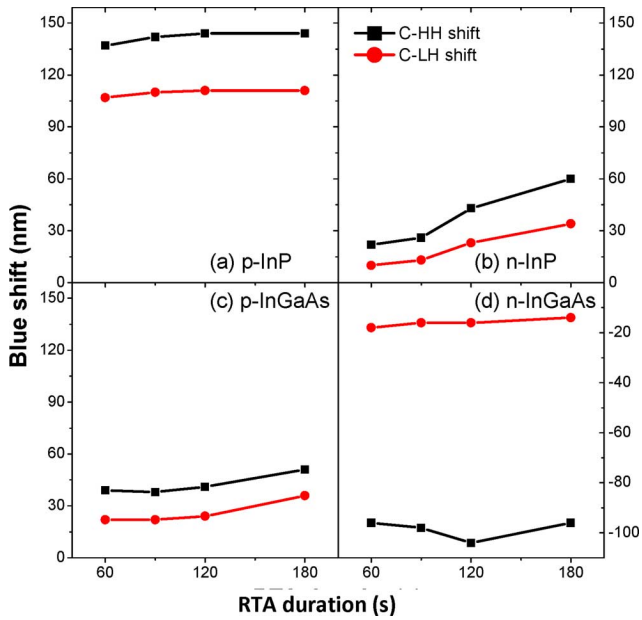

Fig. 5. Measured wavelength shifts versus annealing durations.

observed for the n-InGaAs capped sample. The derived diffusion lengths show big differences among samples, implying different situations of point defect flux from the surface toward the bulk during intermixing, on which the built-in electric field effect [32] plays a role.

The generated near surface point defects are responsible for promoting intermixing in the RTA process, whereas the effect of grown-in defects is negligible as no thermal shift was observed on RTA-only samples at this temperature. The flux of a certain type of point defects J can be expressed as [33]

$$J = -D\left(\frac{\partial N}{\partial x}\right) + z\mu N\varepsilon(x)$$

where N is the defect concentration, D is the diffusion coefficient, z is the defect's charge number, μ is the mobility, and ε is

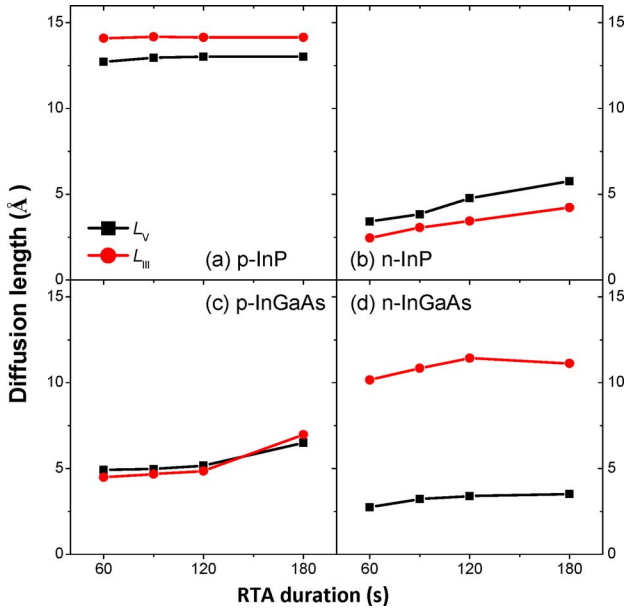

Fig. 6. Derived L_{V} and L_{III} versus annealing durations.

TABLE I
RELATIVE SURFACE COMPOSITIONS OF ICP-PROCESSED InP AND InGaAs-CAPPED SAMPLES MEASURED BY XPS

Sample	III		V		V/III ratio
	In	Ga	As	P	
InP	1.000	/	/	0.843	0.843
$In_{0.53}Ga_{0.47}As$	0.320	0.701	1.000	/	0.979

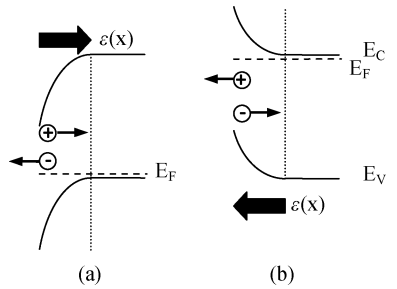

Fig. 7. Sketch of the band-edge profiles for illustrating band bending and its effect on charged point defect diffusion for (a) p- and (b) n-doped cap layers.

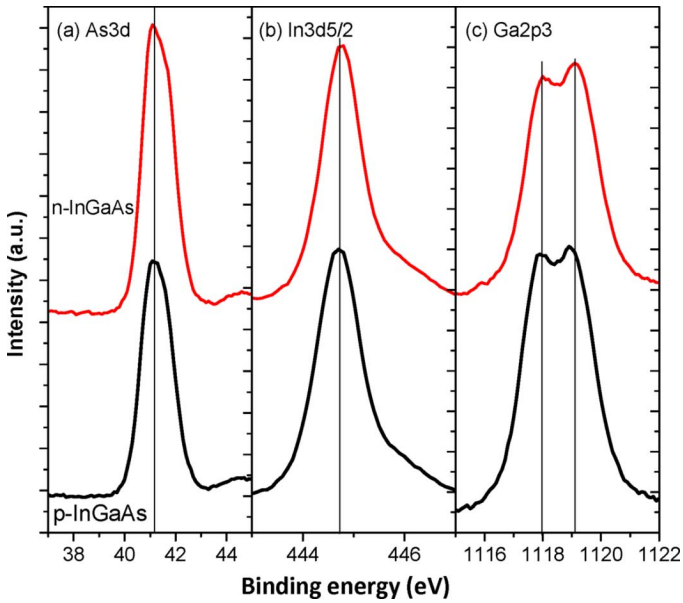

Fig. 8. The As3d In3d5/2 Ga2p3 spectra for p- and n-InGaAs samples after argon plasma treatment.

the electric field. The point defect flux contains a diffusion component due to the concentration gradient and a drift component induced by electric field.

Both n- and p-doped InP encounter band bending due to the Fermi-level (FL) pinning at around 0.4 eV below the conduction band minimum (CBM) after high dosage bombardment at the surface after low-energy argon bombardment. [34]. Due to the pinning of surface FL, positive surface charges are accumulated on the surface, causing band bending and forming a negatively charged depletion region in the near surface for the p-InP cap, while the situation is opposite for the n-InP cap. Band bending leads to an inward and an outward built-in electric field formed near the surface for p- and n-InP, respectively.

For the InP cap layer, point defects are created during the argon plasma process, in which P is preferentially sputtered [35]–[38] to leave an In-rich region within a depth of the order of 150 Å or less [39]. P preferential sputtering is also confirmed in our experiment by X-ray photoelectron spectroscopy (XPS). [15] As shown in Table I, the surface composition is P depleted after 1 min Ar-plasma. As the result of the nonstoichiometric layer adjacent to the surface, the major near-surface point defects are $\mathrm{V_P}$ vacancies and $\mathrm{In_i}$ interstitials for the InP capped samples. The antisite defects are not considered in the discussion as they diffuse much more slowly than vacancies and interstitials. $\mathrm{In_i}$ and $\mathrm{V_P}$ migrate via the kick-out mechanism, i.e., interstitial atoms kick out and replace the congeneric atoms on their crystal sublattice, and vacancies drag neighbouring congeneric atoms on their crystal sublattice. Correspondingly, the diffusions of $\mathrm{In_i}$ and $\mathrm{V_P}$ enhance the intermixing of group III and V atoms, respectively. The $\mathrm{In_i}$ and $\mathrm{V_P}$ in the space charge region of InP are predicted to have $+2/+3$ and $+1$ charge states, respectively, for the FL at -0.4 to -0.6 eV. Obviously, as depicted in Fig. 7, the motion of $\mathrm{In_i}$ and $\mathrm{V_P}$ from the adjacent surface layer to bulk is enhanced by the inward built-in electric field in the depletion region of p-InP, but is suppressed by the outward field in the depletion region of n-InP. This explains the experimental results shown in Fig. 6 that the p-InP sample achieves much greater diffusion lengths than the n-InP sample. Due to the enhancement effect of built-in electric field, the diffusion length of p-InP has already saturated in ~ 60 s when all point defects generated in Argon plasma process are nearly consumed in the annealing process. In contrast, the diffusion length of n-InP still keeps increasing till 180 s, as the consumption of point defects is much slower due to the suppression effect of the built-in electric field.

XPS were investigated on the surfaces of both p- and n-$\mathrm{In_{0.53}Ga_{0.47}As}$ samples that had been processed under argon plasma for 1 min. As shown in Fig. 8, the electron binding energy for As3d, In3d5/2, and Ga2p3 are almost the same for both samples, implying the same surface FL. Therefore, there is a difference in surface band bending (~ 0.75 eV) and thus a difference in built-in electric field near the surface. The surface compositions of $\mathrm{In_{0.53}Ga_{0.47}As}$ samples measured by XPS (see

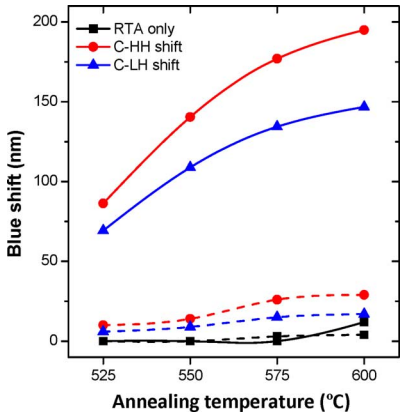

Fig. 9. Measured wavelength shifts versus annealing temperature for p-InP (solid lines) and p-InGaAs (dashed lines) capped samples. The annealing duration is 30 s.

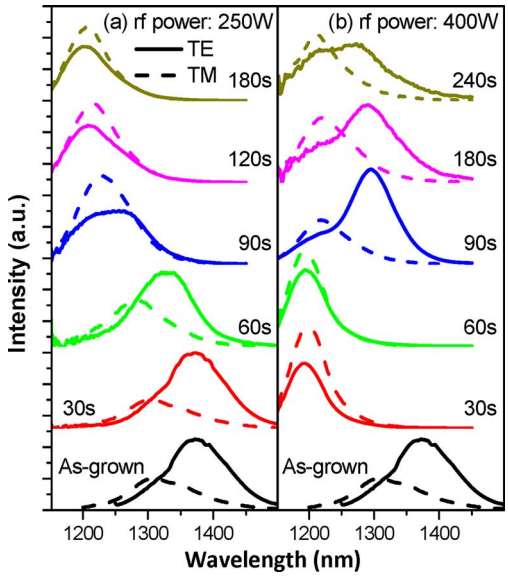

Fig. 10. Measured TE- and TM-PPL spectra of p-InP capped samples for a series of plasma exposure durations and the ICP RF power of 400 and 250 W.

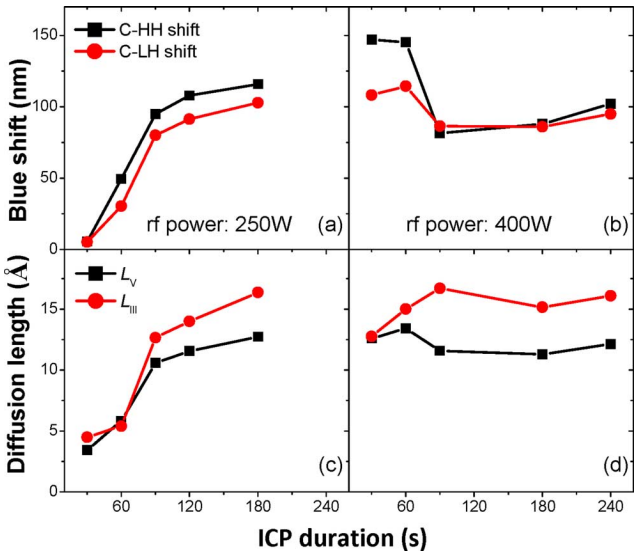

Fig. 11. Measured wavelength shifts and derived L_{V} and L_{III} versus plasma exposure durations with ICP RF power of 400 and 250 W.

Table I) are Ga-riched, which is in agreement with the reported preferential sputtering of In and As in $Ga_{0.73}In_{0.27}As$ in argon plasma process [40]. Therefore, group-III vacancies and Ga_i interstitials can be regarded as major point defects, which benefit interdiffusion on group-III sublattice. The very small L_{V} in both samples shown in Fig. 6(c) and (d) denotes that there are not sufficient group-V near-surface point defects to trigger significant group-V interdiffusion in the given annealing condition. There is a big difference of L_{III} in the two types of samples. The built-in field enhances inward diffusion of negatively-charged group-III vacancies and retards positively charged Ga_i interstitials in the n-InGaAs cap. The situation is opposite in the p-InGaAs cap and group-III vacancies can be annihilated due to recombination with Ga interstitials. Therefore, small L_{III} observed in the latter suggests that negatively charged vacancies are responsible for intermixing on group-III sublattice. This is similar to the conclusion that diffusion occurs via negatively-charged vacancies on group-III sublattice in GaAs. [41]–[45] Red shift observed in the n-InGaAs capped sample is the result of a small V/III diffusion length ratio, but blue shift can be also possible for sufficiently large diffusion lengths, which can be achieved at higher annealing temperature or longer annealing duration [23].

The p-InGaAs cap's deficiency of intermixing capability can be further confirmed in an experiment of annealing of p-InGaAs and p-InP capped samples at a series of temperatures, as shown in Fig. 9. The C-HH blue shifts for the p-InP capped sample are 86 and 195 nm for the lowest and the highest annealing temperatures, respectively. Correspondingly, only 10 and 29 nm are found for the p-InGaAs capped sample. A similar phenomenon that the blue shift was smaller for the InGaAs capped sample than the InP capped sample in ion implantation enhanced QWI was reported, too, but was simply ascribed to the difference in surface amorphorization [46].

V. Plasma Process Influence

For monolithic integration application, large blue shift with short annealing duration and low temperature is preferred to minimize alteration of the structure profile in unwanted areas. In the previous section, we demonstrate that the p-InP is the best cap layer choice for blue shift intermixing. The ICP-enhanced intermixing technique carries out point defect generation and intermixing promotion in separate processes, leaving advantages to process optimization. ICP process may influence the intermixing result via control of process parameters such as plasma exposure duration, plasma power, etc. This section focuses on the investigation of p-InP capped samples with special regards to blue shift control.

Two groups of samples were exposed in Ar-plasma for a series of durations with ICP power fixed at 500 W and RF power set at 250 and 400 W, respectively. RTA process was performed at 550 °C for 30 s. Fig. 10 shows the TE- and TM-PPL spectra for a series of plasma exposure durations with the two RF power settings. As seen in Fig. 11(a) and (c) for the lower RF power, diffusion lengths and blue shifts increase with increasing plasma exposure duration. The density of point defects keep growing in

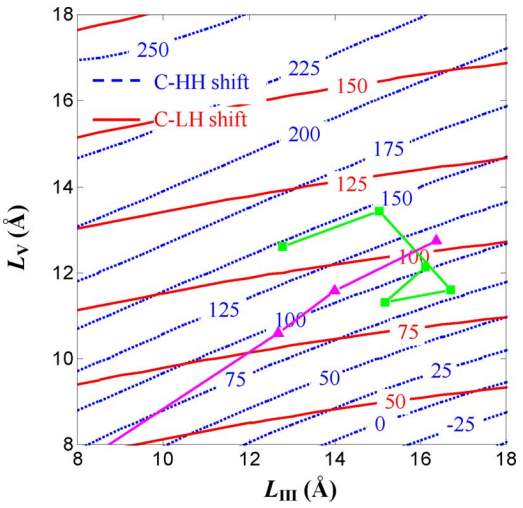

Fig. 12. Contour diagram of C-HH and C-LH wavelength shifts vs L_V and L_{III}. The diffusion length loci for a series of plasma exposure durations with ICP RF power of 400 and 250 W are labeled with square and triangle symbols, respectively.

a wide range of plasma exposure duration. Therefore, the extent of blue shift can also be easily controlled via the exposure time.

Longer Ar-plasma duration, within certain extent, may lead to higher blue shift due to more point defects accumulated near the surface. However, it is also interesting to see a substantial downfall in the blue shift curves, especially for the C-HH case, within $60 \sim 90$ s as shown in Fig. 11(b) for the higher RF power. In this stage, L_V changed a little but L_{III} rose significantly, resulting in a major change in k, i.e., a drop from 0.89 to 0.69. This causes a decrease in blue shift, a phenomenon which can be better understood from the contour diagram in Fig. 12. It is also noticeable that the C-HH and C-LH transition energies were brought closer due to the dominant group-III intermixing in the late stage, i.e., beyond 30-s plasma exposure duration.

The mechanism for point defect accumulation in plasma process is complicated as a result of two competing processes, i.e., creation of defect-rich regime near the surface due to ion bombardment and milling away of the near-surface regime due to sputtering. [47] The V_P and In_i formed in InP due to preferential sputtering are responsible for promoting L_V and L_{III} respectively. However, the overabundance of In near the surface may retard further generation of V_P as the plasma process goes on. Therefore, interdiffusion on group III becomes more intensified. Defect cluster formation in the late stage of plasma process [39], [48], [49] prevents the increase of point defect density and thus the increase of diffusion lengths. This is more obvious for large RF power as seen from Fig. 11.

From the above experiment, we can see that the largest intermixing is achievable with high RF power in short duration. However, the extent of intermixing is more controllable with low RF power, because the blue shift has monotonic response over a wide range of plasma exposure duration. This merit benefits realization of multiple bandgaps in multistep plasma exposure technique [50], whereas both RF power conditions are applicable for other multibandgap techniques such as defect removal [15] or spatial defect modulation [51].

VI. Conclusion

We have investigated argon ICP-enhanced QWI on the quaternary materials InGaAs(P)–InP. PPL characterization is applied for this work as a quantitative analysis method such that the influence of V/III diffusion length ratio can be investigated. P preferential sputtering and built-in field effect play important roles in intermixing. Consequently, the p-InP cap layer is optimal for blue-shift application. Both high and low rf powers are applicable in the ICP process, whereas they are optimal for acquiring maximum blue shift and control of blue shift, respectively. A blue shift as large as 180 nm can be achieved in accompany with a thermal shift of 20 nm only.

References

[1] S. K. Si, D. H. Yeo, K. H. Yoon, and S. J. Kim, "Area selectivity of InGaAsP-InP multiquantum-well intermixing by impurity-free vacancy diffusion," *IEEE J. Sel. Topics Quantum Electron.*, vol. 4, no. 4, pp. 619–623, Jul./Aug. 1998.

[2] C. J. Mclean, J. H. Marsh, R. M. De La Rue, A. C. Bryce, B. Garrett, and R. W. Glew, "Layer selective disordering by photoabsorption induced thermal diffusion in InGaAs/InP based multiquantum well structures," *Electron. Lett.*, vol. 28, pp. 1117–1119, Jun. 1992.

[3] S. Charbonneau, E. S. Koteles, P. J. Poole, J. J. He, G. C. Aers, J. Haysom, M. Buchanan, Y. Feng, A. Delage, F. Yang, M. Davies, R. D. Goldberg, P. G. Piva, and I. V. Mitchell, "Photonic integrated circuits fabricated using ion implantation," *IEEE J. Sel. Topics. Quantum Electron.*, vol. 4, no. 4, pp. 772–793, Jul./Aug. 1998.

[4] A. S. W. Lee, M. MacKenzie, D. A. Thompson, J. Bursik, B. J. Robinson, and G. C. Weatherly, "Enhanced bandgap blueshift due to group V intermixing in InGaAsP multiple quantum well laser structures induced by low temperature grown InP," *Appl. Phys. Lett.*, vol. 78, pp. 3199–3201, May 2001.

[5] S. D. McDougall, O. P. Kowalski, C. J. Hamilton, F. Camacho, B. Qiu, M. Ke, R. M. De La Rue, A. C. Bryce, and J. H. Marsh, "Monolithic integration via a universal damage enhanced quantum-well intermixing technique," *IEEE J. Sel. Topics. Quantum Electron.*, vol. 4, no. 4, pp. 636–646, Jul./Aug. 1998.

[6] H. S. Djie, T. Mei, J. Arokiaraj, and P. Thilakan, "High-density plasma enhanced quantum well intermixing in InGaAs/InGaAsP structure using argon plasma," *Jpn. J. Appl. Phys.*, vol. 41, pp. L867–869, Aug. 2002.

[7] D. Hofstetter, B. Maisenholder, and H. P. Zappe, "Quantum-well intermixing for fabrication of lasers and photonic integrated circuits," *IEEE J. Sel. Topics. Quantum Electron.*, vol. 4, no. 4, pp. 794–802, Jul./Aug. 1998.

[8] J. H. Teng, J. R. Dong, S. J. Chua, M. Y. Lai, B. C. Foo, D. A. Thompson, B. J. Robinson, A. S. W. Lee, and J. Hazell, "Controlled group V intermixing in InGaAsP quantum well structures and its application to the fabrication of two section tunable lasers," *J. Appl. Phys.*, vol. 92, pp. 4330–4335, Oct. 2002.

[9] N. Cao, B. B. Elenkrig, J. G. Simmons, D. A. Thompson, and N. Puetz, "Band-gap blue shift by impurity-free vacancy diffusion in 1.5-μm -strained InGaAsP/InP multiple quantum-well laser structure," *Appl. Phys. Lett.*, vol. 70, pp. 3419–3421, Jun. 1997.

[10] H. S. Djie, C. K. F. Ho, T. Mei, and B. S. Ooi, "Quantum well intermixing enhancement using Ge-doped sol-gel derived SiO_2 encapsulant layer in InGaAs/InP laser structure," *Appl. Phys. Lett.*, vol. 86, pp. 081106–3, Feb. 2005.

[11] S. Barik, H. H. Tan, and C. Jagadish, "High temperature rapid thermal annealing of phosphorous ion implanted InAs/InP quantum dots," *Appl. Phys. Lett.*, vol. 90, pp. 093106–3, Feb. 2007.

[12] H. H. Tan, J. S. Williams, C. Jagadish, P. T. Burke, and M. Gal, "Large energy shifts in GaAs-AlGaAs quantum wells by proton irradiation-induced intermixing," *Appl. Phys. Lett.*, vol. 68, pp. 2401–2403, Apr. 1996.

[13] V. Aimez, J. Beauvais, J. Beerens, D. Morris, H. S. Lim, and B. S. Ooi, "Low-energy ion-implantation-induced quantum-well intermixing," *IEEE J. Sel. Topics. Quantum Electron.*, vol. 8, no. 4, pp. 870–879, Jul./Aug. 2002.

[14] H. S. Djie, J. Arokiaraj, T. Mei, X. H. Tang, L. K. Ang, and D. Leong, "Plasma induced quantum well intermixing for photonic integration," *J. Vac. Sci. Technol. B*, vol. 21, pp. L1–4, Jul./Aug. 2003.

[15] D. Nie, T. Mei, C. D. Xu, and J. R. Dong, "Halftoning bandgap of InAs/InP quantum dots using inductively coupled argon plasma-enhanced intermixing," *Appl. Phys. Lett.*, vol. 89, pp. 131103–3, Sep. 2006.
[16] H. S. Djie, T. Mei, and J. Arokiaraj, "Photoluminescence enhancement by inductively coupled argon plasma exposure for quantum well intermixing," *Appl. Phys. Lett.*, vol. 83, pp. 60–62, Jul. 2003.
[17] D. Nie, T. Mei, H. S. Djie, B. S. Ooi, and X. H. Zhang, "Improving crystal quality of InGaAs/GaAs quantum dots by inductively coupled Ar plasma," *Appl. Phys. Lett.*, vol. 88, pp. 251102–3, Jun. 2006.
[18] H. S. Djie, C. Sookdhis, T. Mei, and J. Arokiaraj, "Photonic integration using inductively coupled argon plasma enhanced quantum well intermixing," *Electron. Lett.*, vol. 38, pp. 1672–1673, Dec. 2002.
[19] C. Sookdhis, T. Mei, and H. S. Djie, "Wavelength monitoring with low-contrast multimode interference waveguide," *IEEE Photon. Technol. Lett.*, vol. 17, no. 4, pp. 822–824, Apr. 2005.
[20] Y. Huang, F. Xia, V. M. Menon, S. R. Forrest, and M. Gokhale, "Reduction of absorption loss in asymmetric twin waveguide laser tapers using argon plasma-enhanced quantum-well intermixing," *IEEE Photon. Technol. Lett.*, vol. 16, no. 10, pp. 2221–2223, Oct. 2004.
[21] H. S. Djie and T. Mei, "Plasma induced quantum well intermixing for photonic integration," *IEEE J. Sel. Topics. Quantum Electron.*, vol. 11, no. 2, pp. 373–382, Mar./Apr. 2005.
[22] M. Schultz, U. Egger, R. Scholz, O. Breitenstein, U. Gosele, and T. Y. Tan, "Experimental and computer simulation studies of diffusion mechanisms on the arsenic sublattice of gallium arsenide," *J. Appl. Phys.*, vol. 83, pp. 5295–5301, May 1998.
[23] D. Nie, T. Mei, X. H. Tang, M. K. Chin, H. S. Djie, and Y. X. Wang, "Argon plasma exposure enhanced intermixing in an undoped InGaAsP/InP quantum-well structure," *J. Appl. Phys.*, vol. 100, pp. 46103–3, Aug. 2006.
[24] H. S. Djie, T. Mei, J. Arokiaraj, C. Sookdhis, L. K. Ang, S. F. Yu, and X. H. Tang, "Experimental and theoretical analysis of argon plasma-enhanced quantum-well intermixing," *IEEE J. Quantum Electron.*, vol. 40, no. 2, pp. 165–174, Feb. 2004.
[25] H. Chen, R. M. Feenstra, P. G. Piva, R. D. Goldberg, I. V. Mitchell, G. C. Aers, P. J. Poole, and S. Charbonneau, "Enhanced group-V intermixing in InGaAs/InP quantum wells studied by cross-sectional scanning tunneling microscopy," *Appl. Phys. Lett.*, vol. 75, pp. 79–81, Jul. 1999.
[26] S. W. Ryu, B. D. Choe, and W. G. Jeong, "Determination of interdiffusion coefficients of cations and anions in InGaAs/InP superlattice," *Appl. Phys. Lett.*, vol. 71, pp. 1670–1672, Sep. 1997.
[27] F. Bollet, W. P. Gillin, M. Hopkinson, and R. Gwilliam, "On the diffusion of lattice matched InGaAs/InP microstructures," *J. Appl. Phys.*, vol. 93, pp. 3881–3885, Apr. 2003.
[28] P. L. Gareso, M. Buda, H. H. Tan, C. Jagadish, S. Ilyas, and M. Gal, "On quantifying the group-V to group-III interdiffusion rates in $In_xGa_{1-x}As$/InP quantum wells," *Semicond. Sci. Technol.*, vol. 21, pp. 829–832, May 2006.
[29] J. E. Haysom, G. C. Aers, S. Raymond, and P. J. Poole, "Study of quantum well intermixing caused by grown-in defects," *J. Appl. Phys.*, vol. 88, pp. 3090–3092, Sep. 2000.
[30] C. D. Xu, T. Mei, and J. R. Dong, "Determination of diffusion lengths for intermixed quaternary quantum well with polarized edge-emitting photoluminescence," *Appl. Phys. Lett.*, vol. 90, pp. 191111–3, May 2007.
[31] P. S. Dobal, H. D. Bistd, A. Manivannan, R. S. Katiyar, S. K. Mehta, and R. K. Jain, "Polarization effects in AlGaAs single quantum well laser structure," *Solid State Commun.*, vol. 100, pp. 337–340, Nov. 1996.
[32] C. D. Xu, T. Mei, M. K. Chin, J. R. Dong, and S. J. Chua, "Built-in electric field enhancement/retardation on intermixing," *Appl. Phys. Lett.*, vol. 91, pp. 181111–3, Oct. 2007.
[33] K. Dev, M. Y. L. Jung, R. Gunawan, R. D. Braatz, and E. G. Seebauer, "Mechanism for coupling between properties of interfaces and bulk semiconductors," *Phys. Rev. B*, vol. 68, pp. 1953111–1953116, Nov. 2003.
[34] Z. W. Deng, R. W. M. Kwok, W. M. Lau, and L. L. Cao, "Band gap state formation in InP $(110)\ldots$ induced by 10 and 100 eV argon ion bombardment," *J. Appl. Phys.*, vol. 86, pp. 3676–3681, Oct. 1999.
[35] J. E. Maslar, P. W. Bohn, D. G. Ballegeer, E. Andideh, I. Adesida, C. Caneau, and R. Bhat, "Structural modification in reactive-ion-etched i-InP and n^+-InP studied by Raman scattering," *J. Appl. Phys.*, vol. 73, pp. 2983–2994, Mar. 1993.
[36] W. M. Lau, R. N. S. Sodhi, and B. J. Finn, "Photoemission study of sputter-etched InP surfaces," *Appl. Phys. Lett.*, vol. 51, pp. 177–179, Jul. 1987.
[37] W. M. Lau, R. N. S. Sodhi, and S. Ingrey, "An x-ray photoelectron spectroscopy study of Fermi level position and surface composition during formation and removal of oxides on InP," *J. Vac. Sci. Technol. A*, vol. 6, pp. 1371–1375, May 1988.
[38] J. S. Pan, A. T. S. Wee, C. H. A. Huan, H. S. Tan, and K. L. Tan, "Argon incorporation and surface compositional changes in InP(100) due to low-energy Ar^+ ion bombardment," *J. Appl. Phys.*, vol. 80, pp. 6655–6660, Dec. 1996.
[39] O. Wada, "Ar ion-beam etching characteristics and damage production in InP," *J. Phys. D*, vol. 17, pp. 2429–2437, Dec. 1984.
[40] G. Padeletti and G. M. Ingo, "Factors determining preferential sputtering in InGaAs system: Angle-resolved small-area XPS investigation," *Surf. Interface Anal.*, vol. 34, pp. 266–270, Sep. 2002.
[41] R. M. Cohen, "Point defects and diffusion in thin films of GaAs," *Mater. Sci. Eng. R*, vol. 20, pp. 167–280, Oct. 1997.
[42] S. B. Zhang and J. E. Northrup, "Chemical potential dependence of defect formation energies in GaAs: Application to Ga self-diffusion," *Phys. Rev. Lett.*, vol. 67, pp. 2339–2342, Oct. 1991.
[43] H. Bracht, "Diffusion in isotopically controlled semiconductor systems," *Physica B*, vol. 274, pp. 981–986, Dec. 1999.
[44] T. Y. Tan and U. Gosele, "Diffusion mechanisms and superlattice disordering in GaAs," *Mater. Sci. Eng. B*, vol. 1, pp. 47–65, Aug. 1988.
[45] R. A. Morrow, "Diffusion in GaAs of a native defect tagged with deuterium," *Appl. Phys. Lett.*, vol. 57, pp. 276–278, Jul. 1990.
[46] C. Carmody, H. H. Tan, and C. Jagadish, "Influence of cap layer on implantation induced interdiffusion in InP/InGaAs quantum wells," *J. Appl. Phys.*, vol. 93, pp. 4468–4470, Apr. 2003.
[47] M. Rahman, "Channeling and diffusion in dry-etch damage," *J. Appl. Phys.*, vol. 82, pp. 2215–2224, Sep. 1997.
[48] J. B. Malherbe and N. G. van der Berg, "Argon bombardment-induced topography development on InP," *Surf. Interface Anal.*, vol. 22, pp. 538–542, Sep. 1994.
[49] J. B. Malherbe and W. O. Barnard, "Preferential sputtering of InP: An AES investigation," *Surf. Sci.*, vol. 255, pp. 309–320, Sep. 1991.
[50] D. Nie, T. Mei, H. S. Djie, M. K. Chin, X. H. Tang, and Y. X. Wang, "Implementing multiple bandgaps using inductively coupled argon plasma enhanced quantum well intermixing," *J. Vac. Sci. Technol. B*, vol. 23, pp. 1050–1053, May/Jun. 2005.
[51] H. S. Djie, T. Mei, J. Arokiaraj, and D. Nie, "Single step quantum well intermixing with multiple bandgap control for III-V compound semiconductors," *J. Appl. Phys.*, vol. 96, pp. 3282–3285, Sep. 2004.

Chengdong Xu received the B.Eng. and Ph.D. degrees from Jilin University, Jilin, China, in 1999 and 2004, respectively.

He is currently a Research Fellow with the School of Electrical and Electronic Engineering, Nanyang Technological University, Singapore. His current research interest is on III-V semiconductor optoelectronics devices.

Ting Mei (M'00–SM'06) received the B.Eng. and M.Eng. degrees in optical engineering from Zhejiang University, China, in 1988 and 1991, respectively, and the Ph.D. degree in electrical engineering from the National University of Singapore, Singapore, in 2000.

He is presently with the School of Electrical and Electronic Engineering, Nanyang Technological University, Singapore. His current research interest is on nanophotonics, semiconductor optoelectronics, low dimensional materials and devices, and nanostructure semiconductor materials.